Effect of Dissolved Gasses on Spray Evaporative Cooling with Water

S.C. Tinker & M. di Marzo

Mechanical Engineering Department, University of Maryland, College Park, MD 20742

Abstract

An experimental investigation of the effect of non-degassed water used to cool a solid surface is presented. The solid surface is subjected to thermal radiant input from three panels positioned above it. The water is deposited on the surface in the form of a sparse spray with droplets of about 10 μl. Previous experiments with degassed water are compared with these new experiments and the effect of dissolved gasses is quantified in terms of the overall transient thermal behavior of the solid. A lower steady-state average temperature is achieved when gasses are not removed from the water. This result suggests that the configuration of the liquid droplets on the surface is different and that the radiant heat input into the droplet is altered by the gas bubbles present in the deposited droplet. This information provides guidance in practical applications such as sprinkler suppression systems where water damages are a concern.

Keywords: water, spray, cooling, dissolved gasses.

Introduction

Evaporative cooling of hot solid surfaces is a desirable heat transfer process in a number of engineering applications. A sparse spray of water deposited on a solid surface allows for large amounts of heat to be removed due to the high latent heat associated with the evaporation of water. Industrial uses for spray cooling include the quenching of molten metals during casting and the coating of surfaces to form protective finishes. Spray and mist cooling find a variety of uses in the power generation industry, such as the cooling of turbine blades and cooling tower applications. In the area of fire suppression and protection, sparse spray cooling finds numerous uses. These include fire suppression in nuclear power plants, in process chemical storage, and in fuel storage facilities.

Several researchers have focused their attention to the fundamentals of the evaporation of droplets and their cooling effects. Simon and Hsu [1] studied the wetting characteristics of evaporating droplets on various surfaces. They recorded droplet shape histories at room temperature on copper, lucite, and teflon surfaces. Both Toda [2] and Bonacina et al. [3] performed early investigations of spray-surface interactions and provided fundamental insight into the uses of mist cooling. Photographic techniques were employed by Zhang and Yang [4] to determine flow patterns in evaporating droplets on glass and copper plates.

The present work constitutes part of a research effort to quantify and develop models for spray cooling of hot solid surfaces in a fire environment. In 1989, diMarzo and Evans [5] modelled a single droplet evaporating on a high thermal conductivity surface. Subsequently,

a theoretical model using boundary element methods to predict the cooling of a semi-infinite solid due to an evaporating droplet was developed by diMarzo et al. [6]. Both a high and a low thermal-conductivity surface heated from below by conduction were studied. In 1993, Tartarini et al. [7] predicted the transient thermal behavior of a solid caused by the evaporation of a single droplet and proposed a model for the impingement of a sparse spray of droplets. Experimental techniques based on infrared thermography to record the evaporation of a droplet on a radiantly heated semi-infinite solid were developed in 1992 by diMarzo at al. [8]. Dawson and diMarzo [9] extended this experimental work to record the effects of a random distribution of droplets (spray) on the surface. In both cases, the solid exhibited low thermal-conductivity. Computer models of the evaporation of a single droplet for radiative heat input conditions are contributed most recently by White et al. [10] and by Tartarini and diMarzo [11].

The research presented here expands on Dawson's investigation of the cooling of a solid surface by multiple droplets evaporation under radiant heat input. While Dawson used deionized and degassed water in his experiments, the experiments in this work used deionized water which has not been degassed. Therefore, the dissolved gasses are at equilibrium with the air at atmospheric conditions. The purposes of this study are: a) to examine both the temporal and spatial behavior of the surface temperature of a low thermal conductivity, semi-infinite solid subjected to radiant heat input and to a sparse spray of non-degassed, deionized water; and b) to compare these results with the similar ones employing degassed water in order to quantify the effect of dissolved gasses.

Experimental Apparatus

The experimental apparatus is shown in Figure 1. The solid is made of Macor, a glass-like material, and it is square in shape with 15.2 cm sides and 2.54 cm thickness. Table 1 lists the relevant thermophysical properties of Macor. As it can be seen, Macor exhibits a relatively high emissivity and a relatively low thermal conductivity. It also has the ability to withstand high thermal stresses, resulting in a smooth, crack-free surface. The Macor tile is mounted on a chilled plate. The purpose of the chilled plate is to hold the lower surface of the tile at a constant temperature of approximately 30 °C. This is achieved by circulating cold water through the plate. The Macor tile is attached to the chilled plate using silicone heat sink compound.

Three radiant panels are used to heat the solid surface. Two of these panels are positioned above the surface at an angle of 30° and symmetric to the vertical axis through the center of the tile. The third panel surrounds the perimeter of the tile to provide uniform heating to the sides of the Macor tile. An infrared camera, located above, focuses on the solid surface and records its transient thermal behavior. The camera looks through a chilled pipe that is used to absorb stray reflections. A droplet dispenser hangs vertically above the surface and works with a positioning mechanism to provide the droplet distribution on the surface. The motivation for using the radiant heat panels (to provide the heat input to the solid surface) is to simulate a fire environment more realistically. The panels may be assumed to radiate as black bodies. Each panel is conical in shape and capable of reaching temperatures in the range of 800 °C. The temperatures of the panels are controlled by an

Omega CN-7100 digital process controller through a feedback loop from the panels. Power to the panels, which are connected in a delta circuit, is supplied by a 208-volt three-phase power supply.

An Inframetrics Model 525 infrared camera detects radiation wavelengths from 8 to 12 microns and translates thermal variations of an object into a real-time, gray image. These images are made up of dark shades that represent cool regions and light shades that represent hot regions. The camera records the thermal image of the surface onto 8 mm videotape using a Sony high resolution VCR. These tapes are stored for the subsequent data processing. The camera uses a 0.61 meter focal length close up lens which is positioned to view a portion of the surface within the droplet impingement region.

Droplet Size and Distribution

The droplet dispenser consists of a tapered, conical, aluminum body with a bored-out central cavity. The cavity exits through a hole at the bottom of the aluminum body. A size 20 IV needle screws into the hole at the bottom of the cavity. The cavity is continuously fed with water from an open reservoir (positioned to provide the desired static head above the dispenser). A plastic diaphragm and an O-ring seal the cavity at its top. A steel piston rests on top of the diaphragm while a solenoid-spacer mechanism is fitted to the top of the piston. When the solenoid is energized, it pushes down on the spacer, causing the piston to deflect the diaphragm and thus eject a droplet from the needle. An average droplet size of 10 $\pm$ 1 μl is obtained with frequencies as high as one Hertz.

In these spray cooling experiments, attempts are made to distribute the droplets in a random fashion over a circular area of the solid surface. To this end, a positioning mechanism consisting of an aluminum plate with a 25.4 cm hole in the center and three moving solenoid-controlled bumpers which collide with and impart motion to the droplet dispenser. The droplet dispenser, which hangs from four cables, swings within the plate hole as it is impacted by the three bumpers. To keep the motion from decaying or falling into a particular pattern, a motorized cam is used to periodically pluck one of the suspension cables.

Figure 2 shows the droplet distribution recorded during a typical experiment. The distribution affects a larger area than the one which is viewed by the infrared camera. The total area that droplets impinge upon is about 3.3 cm in radius. To determine a function approximating this experimental distribution, the motion of the droplet dispenser needs to be characterized. Its motion is limited by the bumpers. The bumpers move in a synchronous fashion in the horizontal plane, with an innermost position that corresponds to a circle with a radius of 1.8 cm and an outermost position that corresponds to a circle with a radius of 3.3 cm. Confined by the motion of the bumpers, the droplet distributer can only move freely in a 1.8 cm radius. The dispenser is never expected to achieve the maximum radial position of 3.3 cm because the bumpers increasingly impede the dispenser as it travels farther from the center of the distribution area. Therefore, the function describing the droplet distribution (namely the fraction of droplet per unit area d at a given radius r) has the following boundary conditions:

1. at r = 0, d(r) = 0 — which ensures that the distribution is proportional to the surface area
2. at r = 0, d'(r) = 2 — which ensures that the distribution is proportional to the surface area
3. at r = h, d'(r) = 0 — which sets a maximum value for the distribution at the normalized radius h bounding the region of free random motion of the droplet dispenser (i.e. h = 0.56)
4. at r = 1, d = 0 — which insures that the outer maximum radial position is never reached
5. $\int_0^1 d\,dr = 1$ — which is the distribution function normalization statement

With these conditions, the function d, describing the droplet distribution is given as:

$$d = 9.15\,r^4 - 22.64\,r^3 + 11.49\,r^2 + 2.00\,r \qquad (1)$$

To check the validity of this result, the function integral is calculated and plotted in Fig. 3 along with the measurements. Error bars of the actual data are also shown. The error bars are determined based on the assumed outermost possible radial position with respect to the outermost droplet. Figure 3 shows that the calculated distribution is in reasonable agreement with the experimental data.

Experimental Procedure

Experiments are run at initial surface temperatures of approximately 110 °C, 130 °C, 150 °C,

160 °C, and 180 °C. At each initial surface temperature, three mass fluxes of non-degassed, deionized water are tested. Over this set of experiments, the mass flux of water ranges from 0.24 g/m^2s to 1.6 g/m^2s. At the higher mass fluxes, the surface is nearing the flooding conditions. The lowest four initial surface temperatures correspond to evaporative cooling, while the highest temperature corresponds to full nucleate boiling for the Macor surface.

The basic procedure followed for each experimental session is described hereafter. The macor surface is cleaned with ethyl alcohol and a soft cloth, lightly rinsed with distilled water, and allowed to dry. The radiant heaters are turned on and heat the surface for approximately two hours prior to experiment initiation. During this time, the solid surface is able to reach a steady state condition. The temperature of the surface is measured using an Omega thermocouple probe (K-type). The infrared camera, power supply, and video equipment are turned on, two hours prior to experimentation in order to minimize thermal drift. The chilled plate and chilled pipe are circulated with water. The droplet dispenser is turned on and allowed 10 to 15 minutes to stabilize at a given frequency which corresponds to a water mass flux. Once stabilized, 50 droplets are collected in a beaker which is quickly capped to avoid evaporation. The beaker and drops are weighed using a Metler electronic balance and the volume of a single droplet is determined. Droplet volumes generally ranged from 9 μl to 11 μl.

After completing the procedures outlined above an experiment for a particular set of conditions begins. First, the initial surface conditions are recorded, then, the droplets

impinge upon the heated surface for a period of twenty-five minutes. During this period the thermal behavior of the surface is recorded by the infrared camera onto 8 mm videotapes.

Data Processing and Reduction

The data processing and reduction for the experiments follow the same procedure adopted by Dawson [9] in his spray cooling experiments using degassed water. After completing an experimental run at a given initial surface temperature, the data recorded by the infrared camera is processed. The real-time, gray images recorded by the camera provide two types of information: a) the transient average temperature of the surface and b) the spatial distribution on the surface at any time. Both analyses employ a video digitization system to obtain the gray-values from a recorded image. A Matrox MVP-AT frame grabber board is installed in an IBM PC-AT and used to digitize single frames into discrete gray-values (one frame every 30 seconds is sampled). Once digitized, each frame can be analyzed pixel by pixel using Imager-AT software linked with user-written source code. For each frame the infrared intensity scale is calibrated using a temperature versus intensity relationship so that shades of gray may be translated into corresponding temperatures.

To determine the transient average surface temperatures frames are digitized at 30-second intervals of a recorded experimental run. There are 130 shades of gray associated with the infrared intensity levels. Since the temperature range is of 100 °C, the temperature resolution is 0.77 °C/ gray-values. The gray-value of every fifth pixel is used over an image

covering a region of 0.046 m x 0.034 m. The average gray-values are then converted into a single average surface temperature.

Spatial distributions of the surface temperature at a specific time are obtained by considering each pixel in a digitized frame individually. Each pixel can be associated with a Cartesian coordinate using knowledge about the viewed area of a frame. The gray-value for each pixel is converted into a temperature, thus yielding a temperature at a particular location on the surface. Again, every fifth pixel is used. Results are plotted in the form of constant temperature contours. The pixels contained in the total viewed area are 512 by 480 in the horizontal and vertical direction, respectively.

Results and Discussion

Contour plots of the temperature distribution on the Macor surface are shown in Figs. 4(a-c) and 5(a-c) for the indicated initial solid surface temperatures and water mass fluxes. Each sequence of plots shows the surface temperature distribution at three different times: a) early in the transient when the surface temperature is close to its initial value; b) further on in the transient, but before steady state conditions have been reached; and c) at or approaching steady state conditions. Results show very distinct locations where droplets are evaporating on the surface, or have just evaporated from the surface and cause a localized cooling effect. At earlier times, the cooling effect due to evaporating droplets is contained within the local region around the droplet. While at later times, the cooling effect on the surface temperature due to individual droplets tend to merge. Also, more droplets

are found on the surface at later times due to the longer evaporation times associated with the decreasing solid surface temperature. Isothermal contours, at lower temperatures, are found near the perimeter of the plot at later times than those found at early times, indicating that the entire surface is cooling. A fluctuation of about ± 2 °C is associated with these plots, due to electronic noise.

Graphical results of the transient average surface temperature are shown in Figs. 6 and 7. The raw data are shown for both the experiments using non-degassed water degassed water [9], respectively. The general trend apparent in each plot for both the degassed and non-degassed data is the decay of the average surface temperature from its initial value to some steady state value. Dawson suggested a fit to the transient temperature data of the form:

$$T = (T_o - T_s)\, e^{-a\,t} + T_s \qquad (2)$$

which is used to curve-fit all the data representing the transient behavior of the average solid surface temperature. The deviation of the data points from a smooth decay occurs due to the nature of the data acquisition. Since only a portion of the sprayed area is viewed and averaged, at any instant, the number of droplets that can be seen may be different than at other instants thus resulting in oscillations of the average surface temperature.

Examination of these results suggests that the dissolved gasses enhance the heat transfer from the surface by decreasing the incoming radiant input and, therefore, achieving a lower steady state temperature. To quantify this effect, one would attempt to relate the variation in the final steady state temperature to the temperature excursion present in the degassed

water results. Two major effects must be included in the characterization of a given transient: a) ΔT, the solid surface temperature drop; and b) θ, the solid surface initial conditions. These quantities are related to the water mass flux and to the radiant heat input respectively. One could suggest to identify, as independent variable, the ratio of these two quantities while retaining the temperature variation as the dependent variable. Table 2 lists the actual numerical values. This analysis would indicate that the effect of dissolved gasses becomes negligible as the values of the ratio $\Delta T / \theta$ increases. This ratio is large for large temperature drops and for initial solid surface temperatures near the onset of nucleate boiling conditions for degassed water. These are the conditions which are most likely in a fire protection situation. Therefore, the dissolved gasses do not affect significantly the evaporative cooling processes associated with fire safety applications.

Note that for temperatures of the solid surface, where nucleate boiling is observed (i.e. for negative values of θ), these conclusions do not apply. The nature of the vaporization phenomena in nucleate boiling is based on a completely different heat transfer mechanism and an extension of the evaporative results or trends is not justified.

Conclusions

Employing a data acquisition system which uses digital image analysis and infrared thermography, the spatial and temporal behavior of the transient surface temperature of a radiantly heated semi-infinite solid cooled by a sparse spray of non-degassed water is recorded and analyzed. The transient thermal behavior is investigated over a range of

different initial surface temperatures and water mass fluxes. The data acquisition system is able to provide information on both the spatial and temporal behavior of the solid in the form of contour plots and transient average temperature plots, respectively.

Contour plots provide a qualitative description of the surface at any instant in time. Results indicate that localized cooling in the region of droplets occurs during the initial impingement of the sparse spray on the surface. At later times, effects of the droplets tend to merge and the average temperature on the surface decreases. More droplets are also found on the surface at later times due to the longer evaporation times associated with the lower surface temperatures.

Transient surface temperature results are compared against those results obtained from experiments using degassed water. In both cases, the surface exhibits an exponential cooling from its initial temperature to some steady state conditions. For larger values of the ratio $\Delta T / \theta$, a smaller difference in the surface cooling between the non-degassed water and the degassed water is observed. These results also indicate that, for low values of the $\Delta T / \theta$ ratio, the dissolved gasses enhance the cooling process by reducing the incoming radiant input.

Acknowledgements

This research has been sponsored by a grant of the Building and Fire Research Laboratory of the National Institute of Standards and Technology.

Nomenclature

a constant

d droplet distribution function

G droplet mass flux

h maximum normalized radius of free random motion of the droplet distributor

r normalized radius (with respect to its maximum possible value of 3.3 cm)

T average solid surface temperature

T_o initial solid surface temperature

T_s final steady state average solid surface temperature

t time

Greek

ΔT solid surface temperature drop, T_o- T_s

θ difference between the initial solid surface temperature at the onset of nucleate boiling for degassed water (~ 163 °C) and the actual initial solid surface temperature

Superscripts

* identifier of properties for degassed water

' identifier of the first derivative with respect to r

References

1. Simon, F. & Hsu, Y.Y., Wetting dynamics of evaporating drops on various surfaces. *NASA Technical Memo*, NASA TM X-67913 (1971).
2. Toda, S., A study of mist cooling. First report: Investigation of mist cooling. *Heat Transfer, Japanese Research*, Vol. 1 (1972) p. 39-50.
3. Bonacina, C., Del Giudice, S., & Comini, G., Dropwise evaporation. *Journal of Heat Transfer*, Vol. 101 (1979) p. 441-446.
4. Zhang, N. & Yang, W.J., Natural convection in evaporating minute drops. *Journal of Heat Transfer*, Vol. 104 (1982) p. 656-662.
5. diMarzo, M., & Evans, D., Evaporation of a water droplet deposited on a hot high conductivity solid surface. *Journal of Heat Transfer*, Vol. 111 (1989) p. 210-213.
6. diMarzo, M., Tartarini, P., Liao, Y., Evans, D. & Baum, H., Evaporative cooling due to a gently deposited droplet. *International Journal of Heat and Mass Transfer*, Vol. 36 (1993) p. 4133-4139.
7. Tartarini, P., Liao, Y. & diMarzo, M., Numerical simulation of multi-droplet evaporative cooling. *Heat and Technology* Vol. 11 (1993) p. 98-107
8. diMarzo, M., Kidder, C.H. & Tartarini, P., Infrared thermography of dropwise evaporative cooling of a semi-infinite solid subjected to radiant heat input. *Experimental Heat Transfer*, Vol. 5 (1992) p. 101-104.
9. Dawson, H. & diMarzo, M., Multi-droplet evaporative cooling: Experimental results. *AIChE Symposium Series*, Vol. 89 (1993) p. 26-35
10. White, G., Tinker, S. & diMarzo, M., Modelling of dropwise evaporative cooling on a

semi-infinite solid subjected to radiant heat input. *Fire Safety Science-Proceedings of the 4th International Symposium*, ed. T. Kashiwagi, Int. Association of Fire Safety Science (1994) p. 217-228

11. Tartarini, P. & diMarzo, M., Dropwise evaporative cooling in radiative field. *Proceedings of the 10th International Heat Transfer Conference*, ed. G.F. Hewitt, Vol. 6 (1994) p. 277-282.

TABLE ONE

Properties of Macor

Density	2,520	kg/m^3
Thermal Conductivity	1.297	W/m-K
Specific Heat	888.9	J/kg-K
Emissivity	0.84	-

TABLE TWO

Gassed-Degassed Water Comparison

Gassed	Degassed	Result	Comparison
ΔT	θ	$\Delta T / \theta$	$T_s - T_s^*$
61	12	5.1	4
41	12	3.4	5
25(29)[a]	32	0.78(0.90)	8(4)
85	1	85	1
40	1	40	0
77	- 19[b]	-	2

[a] The mass flux for the degassed water is 0.5 g/m^2s while the mass flux for the non-degassed water is 0.57 g/m^2s. The quantities in parentheses are prorated to correct for this mass flux discrepancy.

[b] For degassed water, the initial solid surface temperature at the onset of boiling is 163 °C. A negative value of θ indicates thatnucleate boiling is present. θ of -19 °C corresponds to an initial solid surface temperature of 182 °C.

Captions

Fig. 1. Experimental apparatus

Fig. 2. Typical measured droplet distribution

Fig. 3. Comparison of the integrated distribution function *d* and the cumulative measured droplet distribution

Fig. 4. Surface temperature contour plot for T_o = 151 °C and G = 0.96 g/m²s (a: t = 30 s; b: t = 300 s; c: t = 600 s)

Fig. 5. Surface temperature contour plot for T_o = 162 °C and G = 0.97 g/m²s (a: t = 30 s; b: t = 300 s; c: t = 600 s)

Fig. 6. Transient average surface temperature for T_o = 151 °C and G = 0.96 g/m²s (• : non-degassed, fit: $T = 41\ e^{-0.35\,t} + 110$; ▲ : degassed, fit: $T = 46\ e^{-0.34\,t} + 105$)

Fig. 7. Transient average surface temperature for T_o = 162 °C and G = 0.97 g/m²s (• : non-degassed; ▲ : degassed, fit: $T = 40\ e^{-0.40\,t} + 122$ for both sets of data)

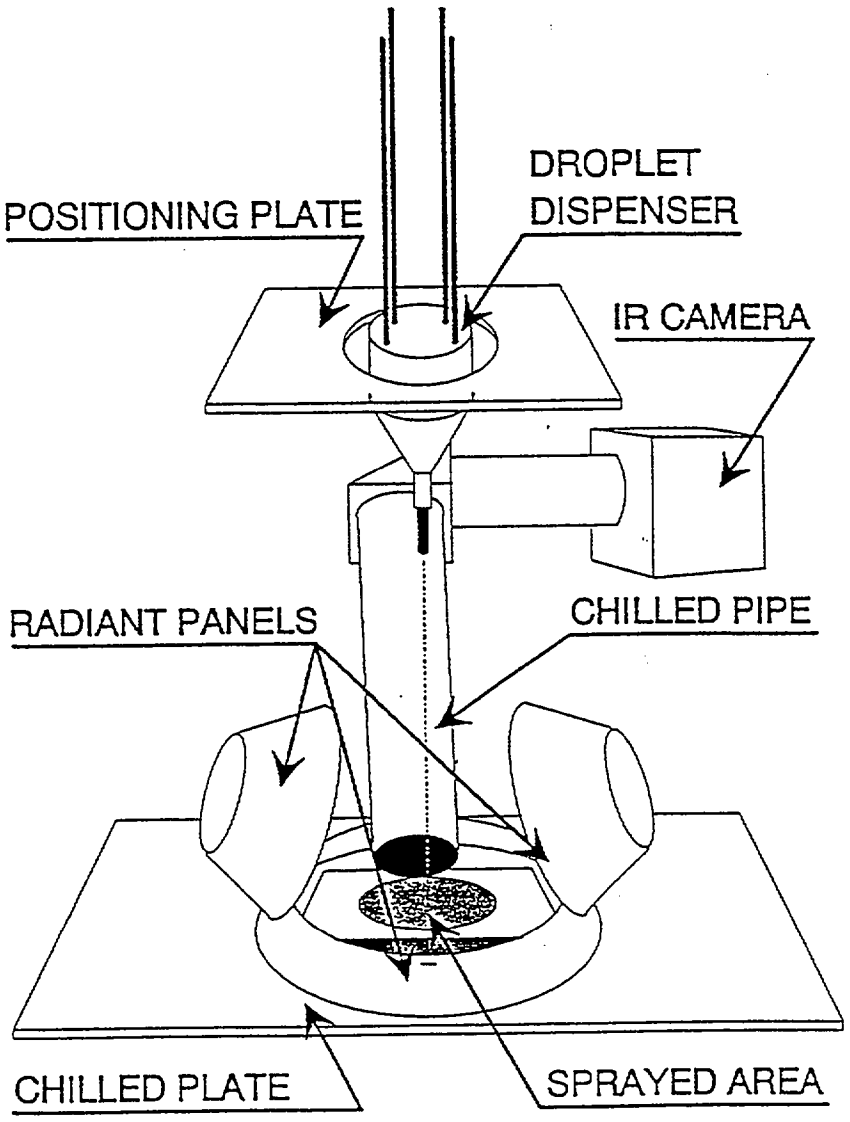
POSITIONING PLATE
DROPLET
DISPENSER
IR CAMERA
RADIANT PANELS
CHILLED PIPE
CHILLED PLATE
SPRAYED AREA

Fig. 1

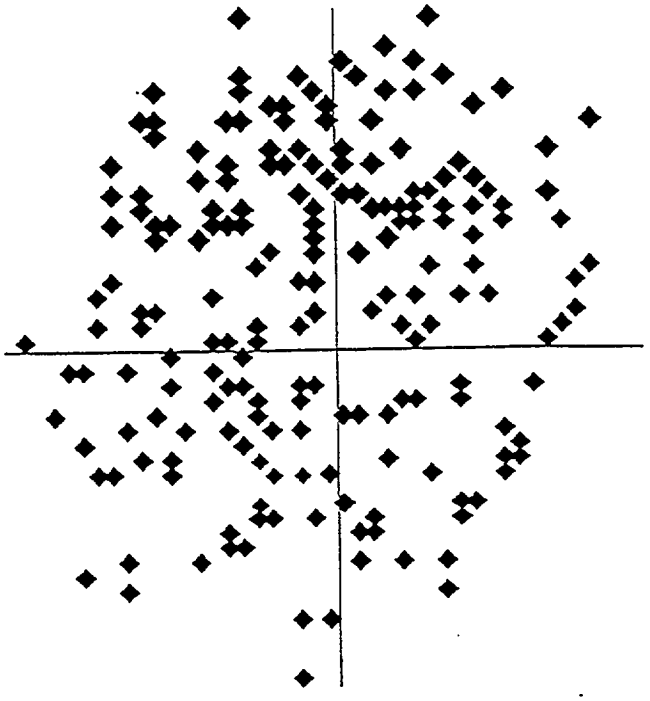

Fig. 2

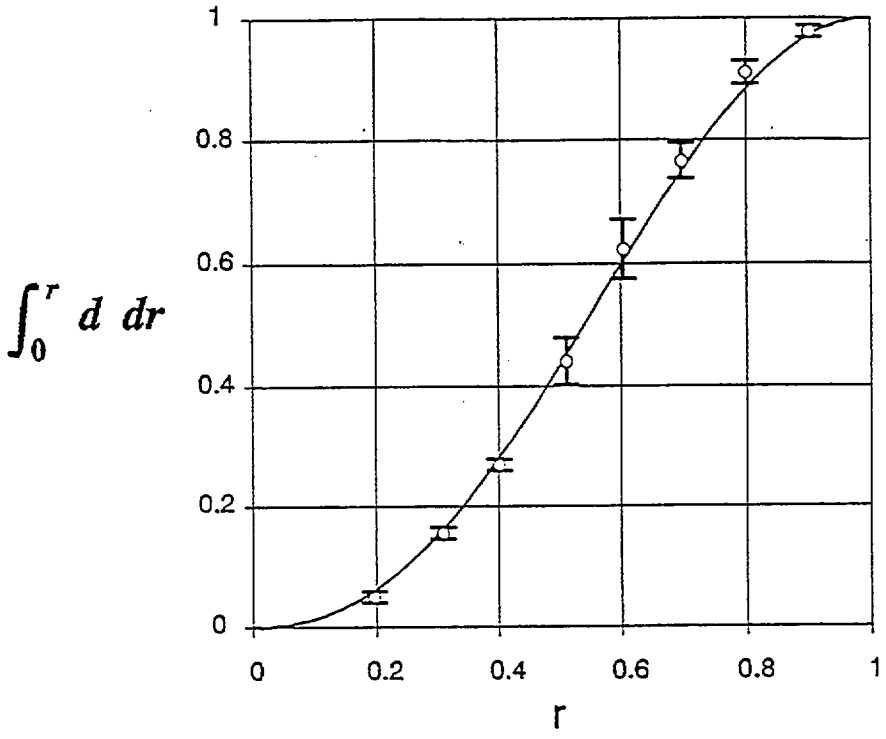

Fig. 3

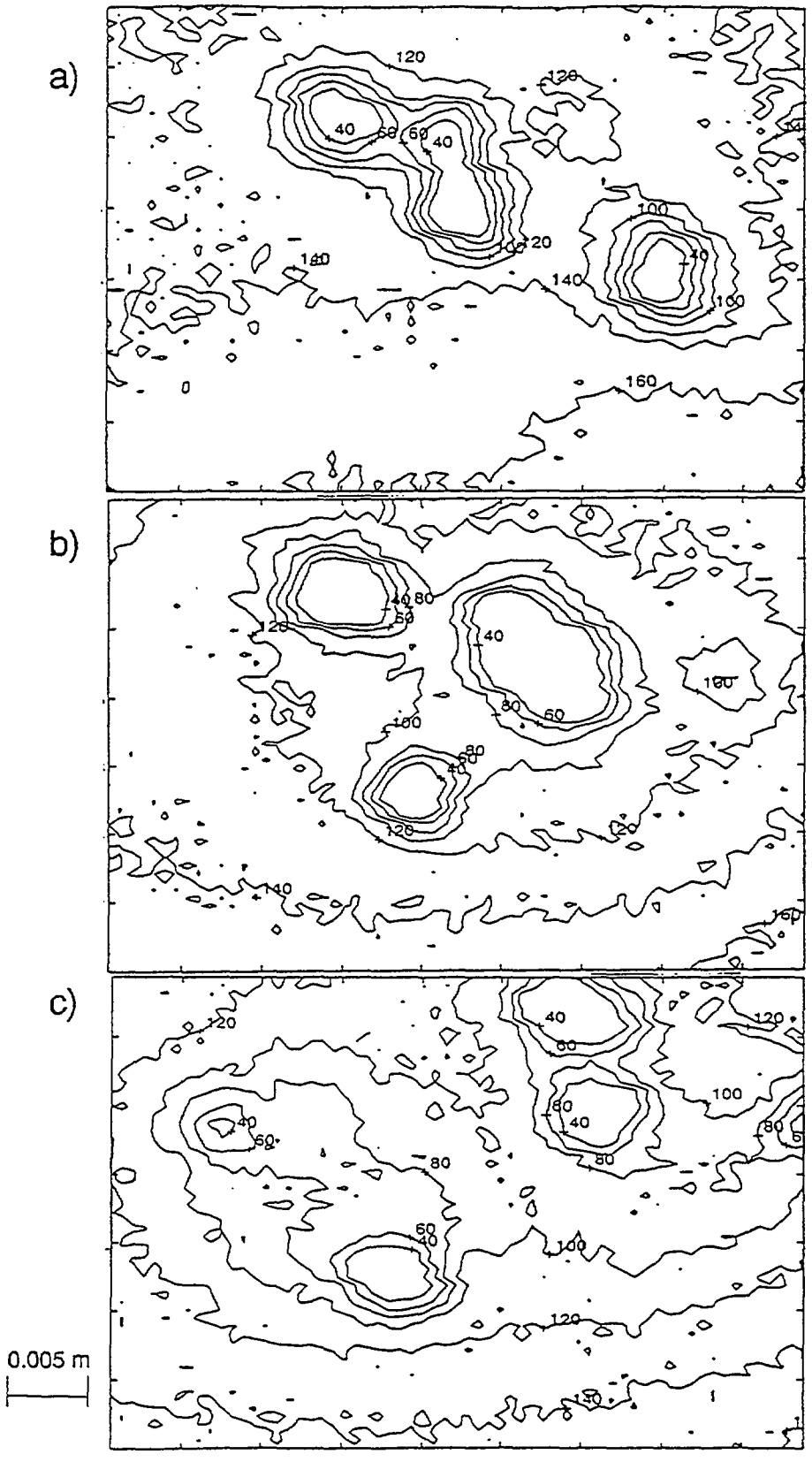

Fig. 4

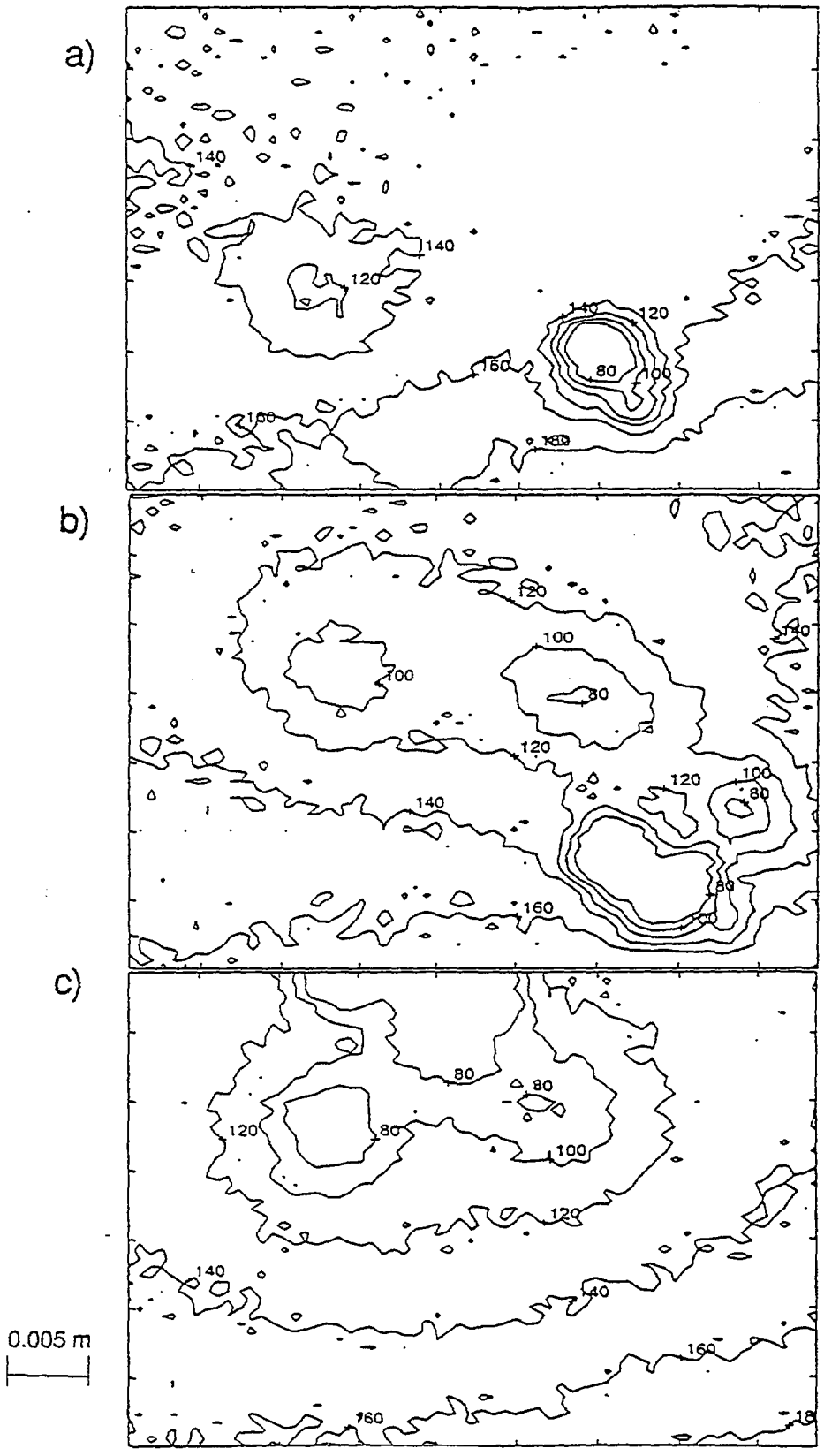

Fig. 5

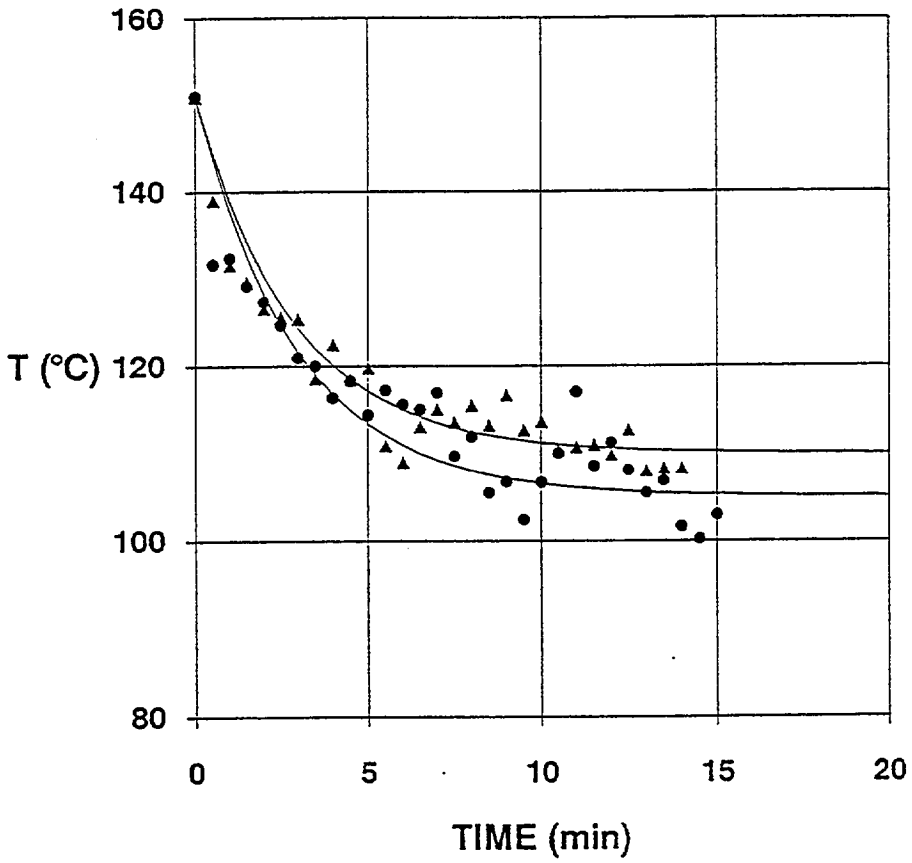

Fig. 6

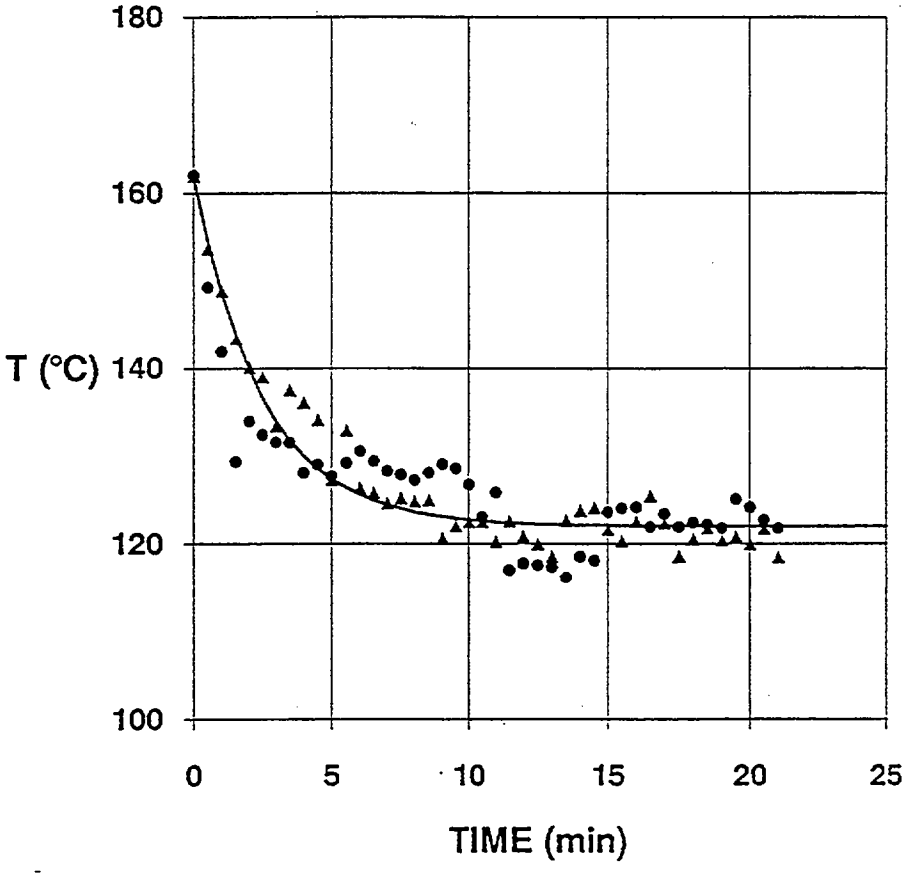

Fig. 7

APPENDIX C:

Criterion for liquid flooding on the solid surface

M. Lederer, M. diMarzo & P. Tartarini, Flooding criterion for evaporative cooling on horizontal semi-infinite solids (1995) unpublished manuscript.